JOURNAL OF MATERIALS SCIENCE 31 (1996) 6609–6614

Solid solutions with rutile structure: electronic behaviour and ultraviolet photoelectron spectrometry study

J. M. BELLOCH, J. ISASI, M. L. LÓPEZ, M. L. VEIGA, C. PICO
Departamento de Química Inorgánica I, Facultad de CC. Químicas, Universidad Complutense de Madrid, 28040-Madrid, Spain

S. FISCHER, W. GOPEL
Institut für Physikalische und Theoretische Chemie, Eberherd-Karls-Universität Tübingen, Auf der Morgentelle 8, D-72076 Tübingen, Germany

Solid solutions of composition $Ti_{2.1}M_{0.3}(Sb_{1-x}Nb_x)_{0.6}O_6$ (M = Co, Ni and Cu) in the range $0 \leq x \leq 1$ are obtained by thermal treatment of the appropriate amounts of simple oxides. The crystal structures have been determined by employing Rietveld structure analysis of powder X-ray diffraction data. Electrical conductivity, magnetic and ultraviolet photoelectron spectrometry (UPS) measurements for these phases are also discussed.

1. Introduction

Rutile is an important structure for many binary oxides MO_2, in which metal is octahedrally (slightly distorted) coordinated to six oxygen, and each anion is in planar three-coordination with metal cations. This structure is built up chains of MO_6 octahedra sharing opposite edges linked to other chains, rotated 90° in the *c* direction, by sharing corners Previous works concerning titanium, antimony and niobium mixed oxides with the general formula $Ti_{2.1}M_xM'_{2x}O_6$ [1–3] have been reported. It was shown that these compounds adopt the rutile or trirutile type structure. Often, certain properties of such materials (magnetic, mechanical, electrical, etc.) can be modified by changing the composition, and it seemed interesting to develop previous knowledge of other solid phases with this structure. Some ternary oxides of the transition elements are currently being investigated as potential candidates for electrodes in solid-state batteries.

In this study $Ti_{2.1}M_{0.3}(Sb_{1-x}Nb_x)_{0.6}O_6$ (M = Co, Ni and Cu, $0 \leq x \leq 1$) solid solutions have been prepared. The structural characterizations of these compounds have been obtained from X-ray powder diffraction and the conductivity and susceptibility magnetic measurements determined on polycrystalline materials. The ultraviolet photoelectron spectrometry (UPS) measurements have allowed information to be obtained on the occupied electronic states of the valence band regions up to the Fermi energy, E_f, but they have not provided a determination of the d^x level's exact position. Moreover, the study carried out by scanning electron microscopy confirms grain-boundary effects to be absent.

2. Experimental procedure

Polycrystalline materials $Ti_{2.1}M_{0.3}(Sb_{1-x}Nb_x)_{0.6}O_6$ (M = Co, Ni or Cu; $0 \leq x \leq 1$), were obtained from a powdered mixture of TiO_2, $M'CO_3$ (M' = Co and Ni) or CuO, Sb_2O_5 and/or Nb_2O_5 (purity $\geq 99.9\%$), in stoichiometric amounts by heating in air from 1423–1523 K for 72 h.

Powder X-ray diffraction patterns were registered at a rate of 0.1° $(2\theta)\,min^{-1}$ by means of a Siemens Kristalloflex diffractometer with a D-500 generator using nickel-filtered CuK_α radiation. A 2θ step size 0.04° was used.

The magnetic susceptibility measurements were made over the temperature range 4.2–300 K using a DMS-5 pendule susceptometer. A maximum magnetic field of 14 kG was applied with $HdH/dZ = 29\,kG^2\,cm^{-1}$. The equipment was calibrated with $Hg[Co(SCN)_4]$ and $Gd_2(SO_4)_3$ and it was independent of the magnetic field in the temperature range used in these experiments.

For the electrical conductivity measurements, the pelletized samples were sintered from 1423–1523 K for 48 h (the sintering temperature was chosen after obtaining a unique slope in the log σ versus $1/T$ graphs). These sintering conditions were established once the measurements were reproducible. The electrical resistivity was measured by using the Van der Pauw method [4]. Contacts were made with platinum paint. The ohmic linear behaviour was established by measuring the current–voltage characteristics, and there was no change in the measured resistivities when the pellet thickness was changed. The Seebeck coefficient was obtained between two points using a Keithley 195A electrometer. In this

0022–2461

measurement, thermal gradients ($\Delta T = 10$ K) were generated and ΔV was obtained on both faces of the sample.

The morphology of the samples was observed by scanning electron microscopy (SEM), using a Jeol JSM 6400.

The UPS measurements were performed in a VSW ultra-high-vacuum chamber with a base pressure of 3.10–10 mbar. For excitation He *I* radiation with an energy of 21.2 eV was used. The excited electrons were detected in a hemispherical electron analyser.

To clean the samples, the system was equipped with an ion sputtering gun (Ar^+ ions). Sample annealing was performed by resistive heating of the tantalum sample holder. All UPS measurements were performed at 570 K to avoid sample charging. The temperatures during heat treatments were monitored with a Ni–CrNi thermocouple. The Fermi energy was determined by taking a spectrum of a clean sputtered silver foil.

3. Results

Under the experimental conditions given above, various rutile-type solid solutions $Ti_{2.1}M_{0.3}(Sb_{1-x}Nb_x)_{0.6}O_6$ have been isolated. The unit cell parameters, c/a ratio and the volume for all the solid solutions, are listed in Tables I–III. X-ray diffraction results were analysed by the Rietveld method [5]. Fig. 1 shows the calculated and theoretical profiles for $Ti_{2.1}Cu_{0.3}(Sb_{0.5}Nb_{0.5})_{0.6}O_6$ as example. In the other compounds, similar results were obtained. The refined atom positions, *R*-factors and bond lengths, obtained from the Fullprof program [6] are listed in Table IV, for $Ti_{2.1}M_{0.3}(Sb_{0.5}Nb_{0.5})_{0.6}O_6$. All metal atoms are randomly distributed in $2a(0, 0, 0)$ sites of the space group $P4_2/mnm$ and the oxygen atoms occupy the $4f(x, x, 0)$ sites. The results of X-ray diffraction for other compositions were similar to those obtained for $x = 0.5$. The TiO_6 octahedra in rutile-TiO_2 exhibit two long Ti–O distances (0.198 nm) and four short Ti–O (0.194 nm) ones. In the same way all the phases are characterized by two longer distances and four short M–O distances.

TABLE I Crystallographic data for the oxides $Ti_{2.1}Co_{0.3}(Sb_{1-x}Nb_x)_{0.6}O_6$

x	a(nm)	c(nm)	c/a	V (10^{-3} nm^3)
0	0.4618(1)	0.3005(1)	0.651	64.0
0.3	0.4625(1)	0.2998(2)	0.648	64.1
0.5	0.4629(2)	0.2995(1)	0.647	64.1
0.7	0.4633(1)	0.2994(1)	0.646	64.2
1	0.4642(1)	0.2987(1)	0.644	64.3

TABLE II Crystallographic data for oxides $Ti_{2.1}Ni_{0.3}(Sb_{1-x}Nb_x)_{0.6}O_6$

x	a(nm)	c(nm)	c/a	V (10^{-3} nm^3)
0	0.4610(1)	0.2995(2)	0.649	63.6
0.3	0.4615(1)	0.2992(1)	0.648	63.7
0.5	0.4619(2)	0.2986(1)	0.646	63.7
0.7	0.4621(1)	0.2985(2)	0.645	63.7
1	0.4632(1)	0.2979(1)	0.643	63.8

TABLE III Crystallographic data for oxides $Ti_{2.1}Cu_{0.3}(Sb_{1-x}Nb_x)_{0.6}O_6$

x	a(nm)	c(nm)	c/a	V (10^{-3} nm^3)
0	0.4615(1)	0.2993(2)	0.648	63.7
0.1	0.4619(1)	0.2992(2)	0.647	63.8
0.3	0.4625(2)	0.2998(1)	0.646	63.9
0.4	0.4626(1)	0.2988(1)	0.645	63.9
0.5	0.4627(2)	0.2989(1)	0.645	63.9
0.7	0.4632(1)	0.2985(2)	0.644	63.9
1	0.4645(1)	0.2989(1)	0.643	64.4

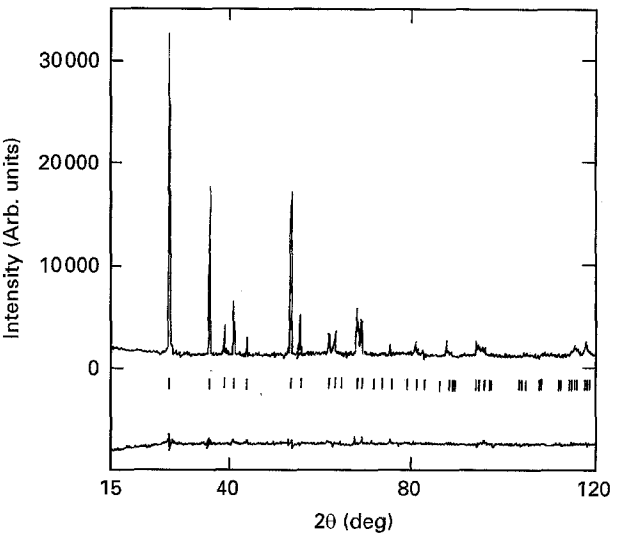

Figure 1 Observed (dots), calculated and difference diffraction profiles for $Ti_{2.1}Cu_{0.3}(Sb_{0.7}Nb_{0.3})_{0.6}O_6$.

Fig. 2 shows that the variation of the reciprocal molar susceptibility, χ_m^{-1} versus T for one of these materials, $Ti_{2.1}Ni_{0.3}(Sb_{0.7}Nb_{0.3})_{0.6}O_6$, is linear, according to the Curie–Weiss law. Similar results have been obtained for the other phases. Experimental magnetic moments obtained for cobalt ($\mu_{exp} \approx 4.20$ BM), nickel ($\mu_{exp} \approx 3.09$ BM) and copper ($\mu_{exp} \approx 1.63$ BM) phases are in good agreement with the calculated ones (3.87, 2.83 and 1.73 BM, respectively) using the spin-only contributions ($S = 3/2$ in Co^{2+}, $S = 1$ in Ni^{2+} and $S = 1/2$ in Cu^{2+}). On the other hand, the Weiss constant is positive for cobalt ($\theta \approx 12$ K), negative for nickel ($\theta \approx -9$ K) and positive for copper ($\theta \approx 60.89$ K) compounds. No interactions between paramagnetic ions takes place.

TABLE IV Reliability factors, *R*, oxygen parameters, x and M–O distances obtained after refinement

		$Ti_{2.1}Co_{0.3}(Sb_{0.5}Nb_{0.5})_{0.6}O_6$	$Ti_{2.1}Ni_{0.3}(Sb_{0.5}Nb_{0.5})_{0.6}O_6$	$Ti_{2.1}Cu_{0.3}(Sb_{0.5}Nb_{0.5})_{0.6}O_6$
R_p		10.9	9.1	5.55
R_{wp}		14.4	12.1	7.70
R_b		3.99	5.74	6.53
x		0.3045	0.3023	0.3024
d_1(M–O)×2	(nm)	0.1996	0.1977	0.1987
d_2(M–O)×4	(nm)	0.1968	0.1967	0.1979

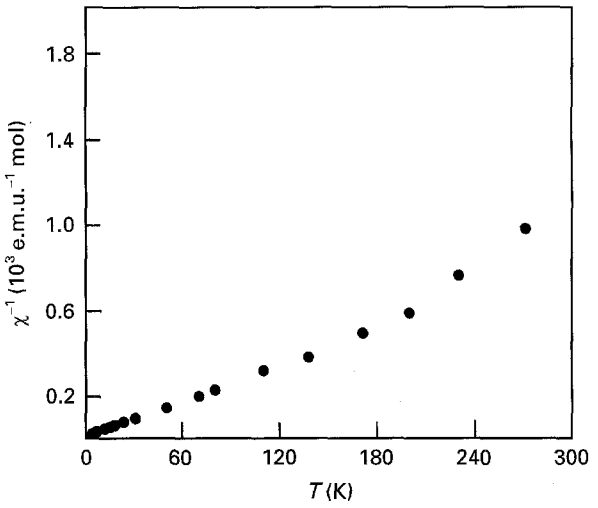

Figure 2 Variation of magnetic susceptibility, χ_m^{-1} with temperature for $Ti_{2.1}Ni_{0.3}(Sb_{0.7}Nb_{0.3})_{0.6}O_6$.

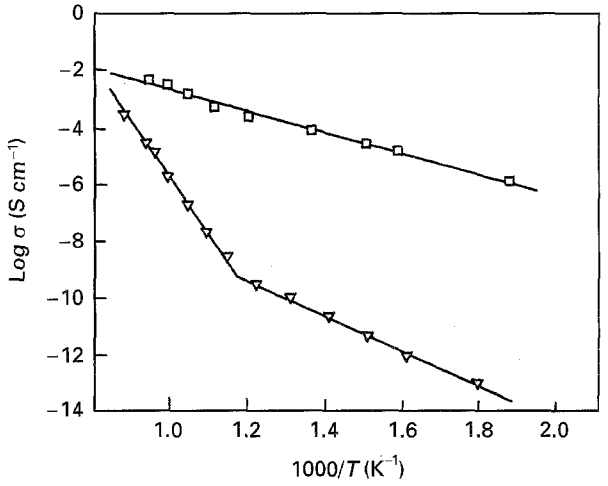

Figure 3 Variation of log σ with 1000/T for $Ti_{2.1}Ni_{0.3}Nb_{0.6}O_6$: (▽) 24 h, E_a = 1.56 and 0.80 eV; (□) 48 h, E_a = 0.64 eV.

The conductivity measurements were carried out on pressed pellets for the compositions $x = 0$–1. In order to analyse the influence of sintering temperature on the conductivity measurements in these series, as an example, the conductivity data were determined for one sample, which was sintered at 1423 K for 24 or 48 h. Fig. 3 shows Arrhenius plots of the logarithm of conductivity versus 1000/T. It can be observed clearly that the thermal treatment for 24 h leads to two values of the activation energy, which are roughly related to the grain boundary (higher E_a) and bulk (lower E_a) contributions. Only one slope is obtained (E_a = 0.64 eV) for the 48 h sintered sample. Those results suggest that the most appropriate treatment for the materials is around 1423 K for 48 h.

The way in which the grain-boundary structure can affect the conductivity is illustrated in the following example. Typical scanning electron micrographs of $Ti_{2.1}M_{0.3}Nb_{0.6}O_6$ (M = Co, Ni and Cu) that were sintered at 1423 K, for 48 h, are shown in Fig. 4. Clearly visible features are the inhomogeneous grains and the thin grain-boundary film, marked by triangles in the micrograph for the nickel and copper solid

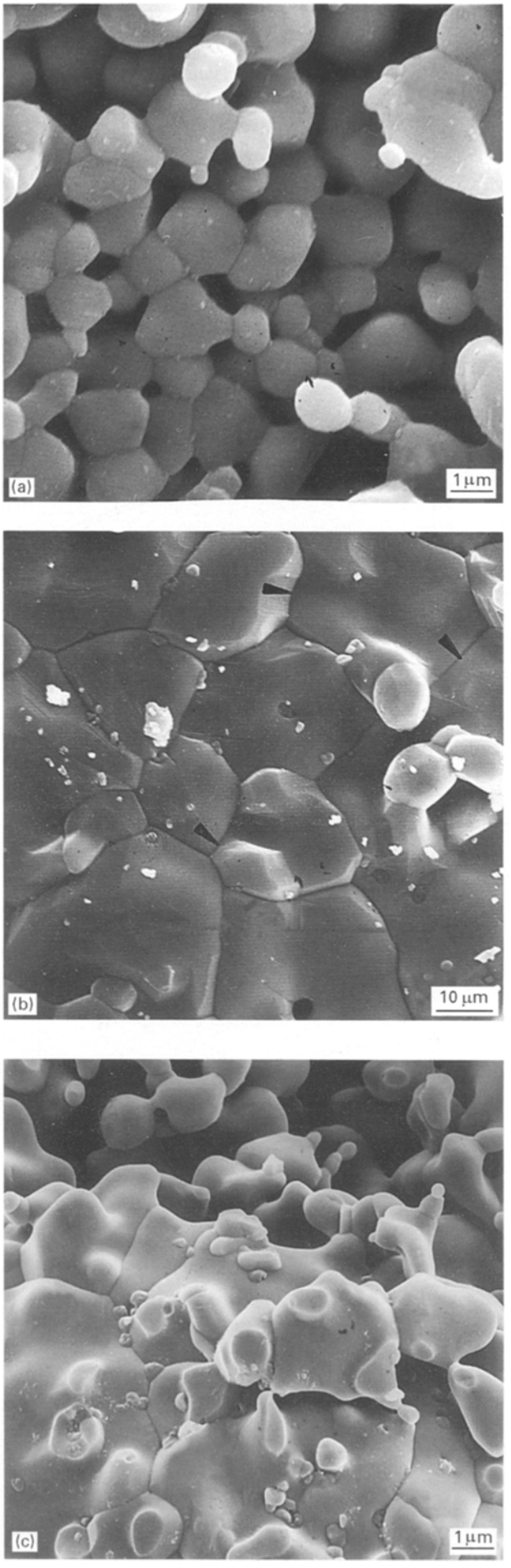

Figure 4 Scanning electron micrographs of the oxides: (a) $Ti_{2.1}Co_{0.3}Sb_{0.6}O_6$ (b) $Ti_{2.1}Ni_{0.3}Nb_{0.6}O_6$ and (c) $Ti_{2.1}Cu_{0.3}Nb_{0.6}O_6$ showing continuous grain-boundary phase.

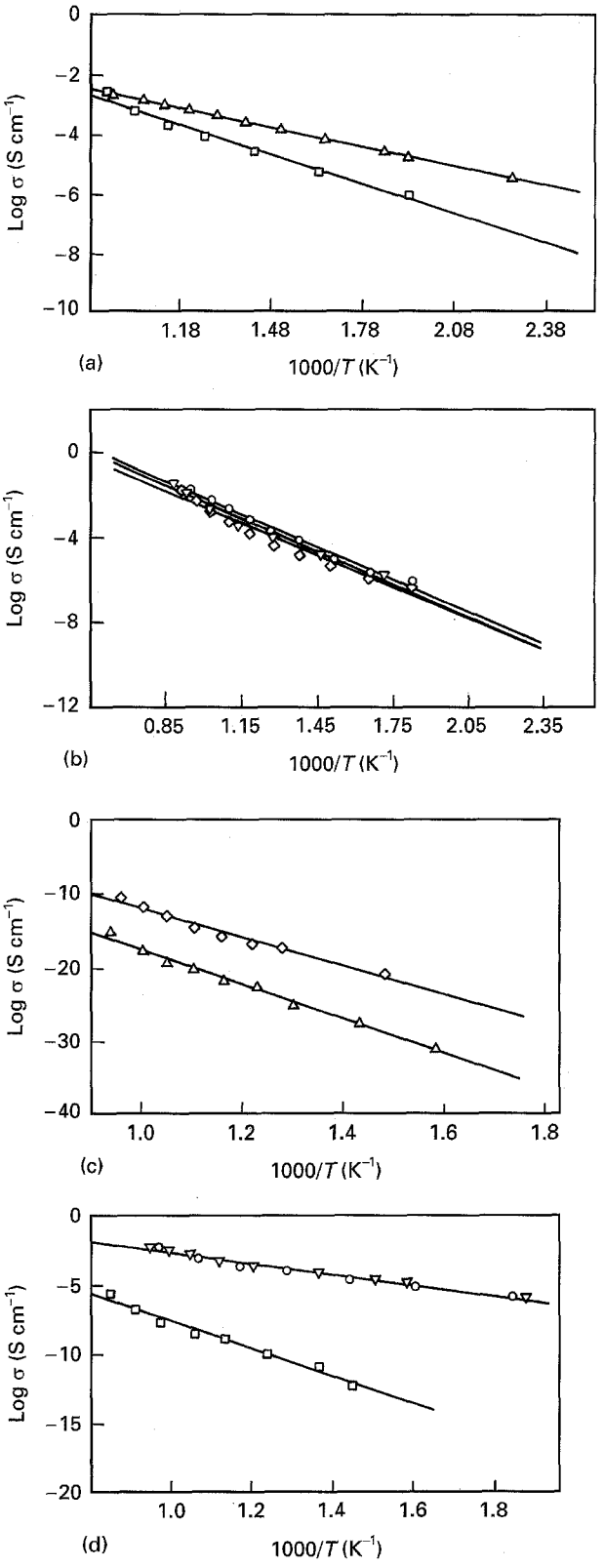

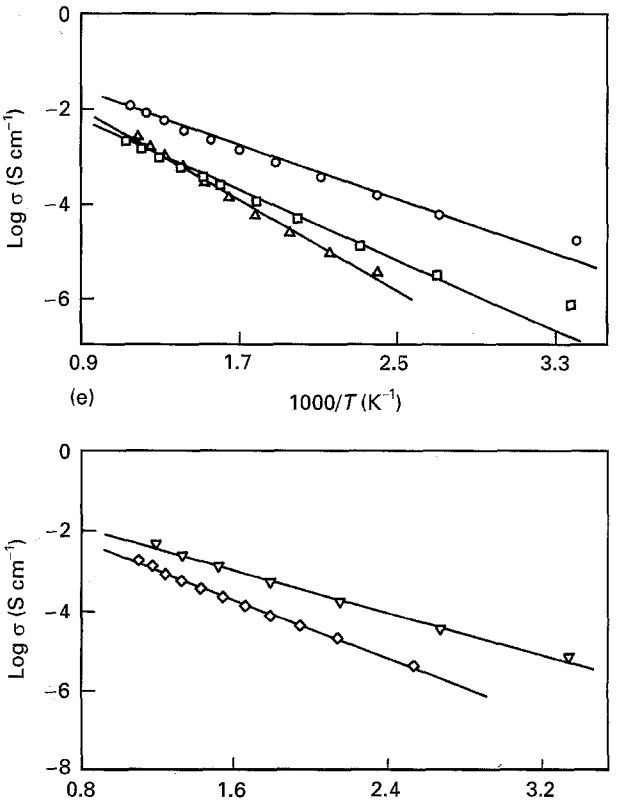

Figure 5 Variation of log σ with 1000/T for solid solutions: (a, b) $Ti_{2.1}Co_{0.3}(Sb_{1-x}Nb_x)_{0.6}O_6$, (c, d) $Ti_{2.1}Ni_{0.3}(Sb_{1-x}Nb_x)_{0.6}O_6$, (e, f) $Ti_{2.1}Cu_{0.3}(Sb_{1-x}Nb_x)_{0.6}O_6$. x: (a) (△) 0, (□) 0.3; (b) (▽) 1, (○) 0.7, (◇) 0.5; (c) (◇) 0.5, (△) 0; (d) (▽) 1, (○) 0.7, (□) 0.3; (e) (○) 0.7, (□) 0.3; (△) 0; (f) (▽) 1, (◇) 0.5.

TABLE V Activation energies

Activation energy (eV) x	M = Co	M = Ni	M = Cu
0	0.47	0.86	0.47
0.3	0.65	0.80	0.35
0.5	0.98	0.70	0.34
0.7	0.99	0.64	0.28
1	1.01	0.64	0.25

solution (Fig. 4b and c). However, in the cobalt oxide (Fig. 4a), the grains are homogeneous and the particle size is smaller than in other oxides, although the grain boundary appears to be discrete, allowing a good intergranular contact.

Fig. 5 shows the variation of log σ with reciprocal temperature for solid solutions of cobalt, nickel and copper, respectively. The curves follow the well-known exponential relation $\sigma = \sigma_0 \exp(-E_a/KT)$. From the obtained results, it can be deduced that these oxides show a typical semiconductor behaviour.

The values of the activation energies, E_a, deduced from log σ versus T^{-1} are given in Table V. Activation energies for solid solutions of nickel and copper decrease when the Nb^{5+} content increases. However, for solid solutions of cobalt, this behaviour is reversed and for, the highest amounts of Nb^{5+}, the materials are practically insulators (Table V) from $x = 0.5$.

The results obtained from UPS shown in Fig. 6 are indicative that all materials are semiconductors because there is no electron density at the Fermi level. The electron density that is due to the O 2p valence band has two maxima at 8 and 5 eV binding energy. These maxima correspond to bonding and antibonding O 2p orbitals [7].

The valence band maximum is located at 3.5 eV below the Fermi level for all compounds. Beyond the valence band maxima, we find electron density in the band-gap region which can be separated in two states with binding energies of 2.5 and 1.3 eV. These states which cannot be found in the stoichiometric TiO_2 (rutile) [7] come from either of the doping compounds

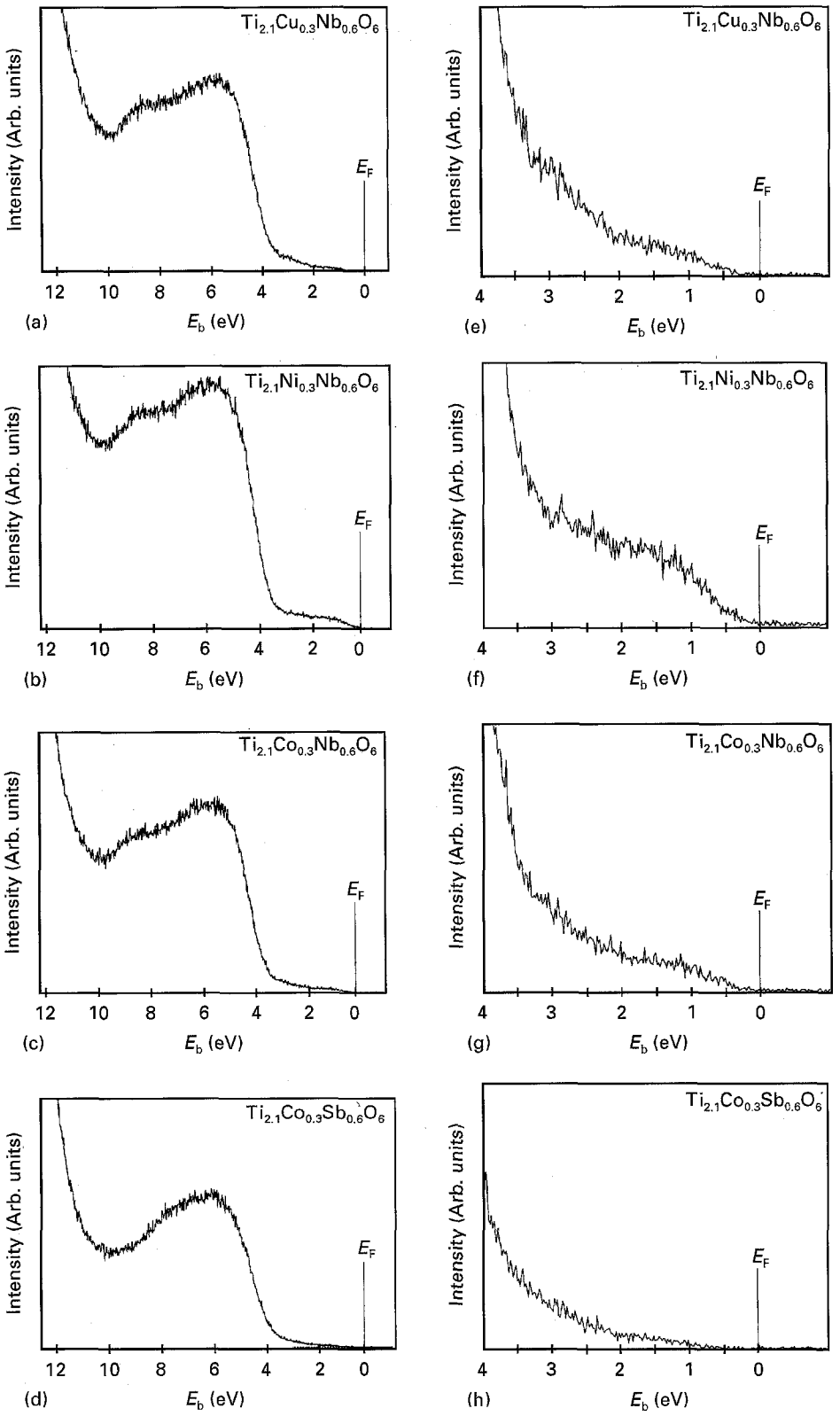

Figure 6 (a–d) The four UP (He *I*)-spectra showing the valence band regions of the different semiconducting materials. (e–h) The enlarged regions close to the Fermi energy. All spectra were taken at 570 K to avoid sample charging.

(metallic d-states). These results are observed in reduced TiO_2 [7].

The activation energy values obtained from the electric measurements indicate that it is not possible to verify these values with the UPS results. However, it can be seen that the highest occupied orbitals have binding energies of 0.5 eV. If we claim that the E_a values obtained from the electric measurements are correct, the conduction band should be located directly over the E_f. This would mean that the gap between valence band and conduction band is around 3.5 eV.

A different behaviour with respect to a reduced signal intensity of the O 2p valence band and the band-gap states and a less structured O 2p valence band signal can be observed for the antimony

compound. These effects might be due to slight sample charging at temperatures up to 570 K. At temperatures of 720 K, a well-structured O 2p valence band can be observed, but the intensity of both the O 2p signal and the band-gap states did not change compared with the spectrum taken at 570 K. So these findings may lead to the conclusion that the antimony compound has less conductivity compared to the other three semiconductors.

In a previous report [8] we established that the cobalt compounds are p-type and the nickel oxides n-type semiconductors. These results could be explained taking into account the band model developed by Goodenough [9] for the rutile-type oxides. We think that the conduction band is mainly formed from $3d$ titanium orbitals and the valence band by $2p$ oxygen orbitals and we assume that d^x transition cation levels can be located between the valence and conduction bands [1]. For the d^7 (Co^{2+}) configuration a t_{2g} level is half-filled ($t_{2g}^5 e_g$) and it can act as an acceptor level above the top of the valence band. Moreover, the more electronegative character of the antimony with respect to niobium would allow the $4d^{10}$ levels to be located in the valence band. This fact explains why this solid solution has insulator behaviour when the Nb^{5+} content increased. For the Ni^{2+} (d^8) and Cu^{2+} (d^9) compounds, half-filled levels are now the e_g ones. These levels could act as donors and promote electrons into the conduction band and these compounds are better conductors when the Nb^{5+} content is increased.

Acknowledgements

We are indebted to the CICYT (MAT 94-079) and DGICYT (PB 92-0214) for financial support.

References

1. E. RAMOS, I. AIVAREZ, M. L. LOPEZ, M. L. VEIGA, M. GAITAN, C. PICO, J. SORIA and A. JEREZ, *Mater. Res. Bull.* **27** (1992) 1431.
2. E. RAMOS, M. L. VEIGA, F. FERNANDEZ, R. SAEZ-PUCHE and C. PICO, *J. Solid State Chem.* **91** (1991) 113.
3. M. GREENBLA, K. RAVINDRON NAIR, W. H. McCARROLL and J. V. WASZCZAK, *Mater. Res. Bull.* **19** (1984) 777.
4. J. VAN DER PAUW, Philips Research Report (1958) p. 1.
5. H. M. RIETVELD, *J. Appl. Crystallog.* **16** (1983) 183.
6. R. RODRIGUEZ-CARVAJAL, "Fullprof" program, ILL Grenoble, France (1993).
7. ZHAOMING ZHAN, SHIN-PUU JENNG, V. E. HENRICH, *Phys. Rev.* **B43** (1991) 12004.
8. J. M. BELLOCH, J. ISASI, M. L. LOPEZ, M. L. VEIGA and C. PICO, *Mater. Res. Bull.* **29** (1994) 861.
9. J. B. GOODENOUGH, "Les oxides des métaux de transicion" (Gauthier-Villars, Paris, 1973).

Received 13 April 1995
and accepted 13 February 1996